Contribution from the Department of Chemistry,
Northwestern University, Evanston, Illinois 60208

Synthesis, Structure, and Stereochemical Analysis of $[PPN][Fe_4(CO)_{13}(HgMo(CO)_3Cp)]$ and $[PPN][Fe_4(CO)_{13}(HgFe(CO)_2Cp)]$

Jiandang Wang, Michal Sabat, Colin P. Horwitz, and Duward F. Shriver*

Received July 27, 1987

Compounds $[PPN][Fe_4(CO)_{13}(HgMo(CO)_3Cp)]$ and $[PPN][Fe_4(CO)_{13}(HgFe(CO)_2Cp)]$ ($[PPN]^+$ = bis(triphenylphosphine)-nitrogen(1+) and Cp = cyclopentadienyl) were synthesized by coordination of the Lewis acid ligand $[HgMo(CO)_3Cp]^+$ or $[HgFe(CO)_2Cp]^+$ to $[PPN]_2[Fe_4(CO)_{13}]$. A single-crystal X-ray structure determination demonstrates that $[Fe_4(CO)_{13}(HgMo(CO)_3Cp)]^-$ (**3**) is a four-iron butterfly cluster ion containing a Π-CO ligand. The Lewis acid is coordinated to the hinge of the butterfly. In solution, spectroscopic data indicate the presence of the butterfly form as well as an isomer having a tetrahedral four-iron array. A higher butterfly to tetrahedral isomer ratio was observed for solutions of **3** than for a previously studied analogue containing a less bulky Lewis acid ligand, $[Fe_4(CO)_{13}(HgCH_3)]^-$ (**5**). From the temperature dependence of the isomer ratio of **3** and **5**, values of $\Delta H°$ and $\Delta S°$ were determined for the butterfly to tetrahedron equilibrium. Carbonyl stretching frequency and isomer ratio data on **3** and similar compounds indicate that the $[HgMo(CO)_3Cp]^+$ ligand induces the butterfly configuration through electronic demand on the cluster as well as through steric bulk. Crystal data for the $[PPN]^+$ salt of **3**: triclinic, a = 16.174 (4) Å, b = 18.457 (4) Å, c = 10.995 (2) Å, α = 100.22 (2)°, β = 105.57 (2)°, γ = 64.77 (2)°, $P\bar{1}$, Z = 2, final R = 0.036, R_w = 0.051.

Introduction

The four-iron carbonyl cluster $[Fe_4(CO)_{13}]^{2-}$ (**1**) was first synthesized as the $[Fe(C_5H_5N)_6]^{2+}$ salt in Walter Hieber's laboratory in 1930, and its protonated derivative $[Fe_4(CO)_{13}(H)]^-$ (**2**) was reported from the same laboratory in 1957.[1,2] X-ray

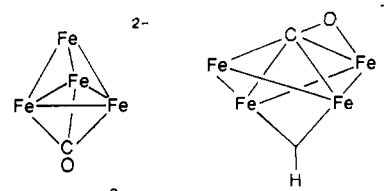

$[Fe_4(CO)_{13}]^{2-}$ (1) $[Fe_4(CO)_{13}(H)]^-$ (2)

crystal structure determinations establish that $[Fe_4(CO)_{13}]^{2-}$ (**1**) consists of a tetrahedral array of iron atoms[3] and that $[Fe_4(CO)_{13}(H)]^-$ (**2**) contains a butterfly array of iron atoms with a Π-CO group.[4] Subsequent variable-temperature multinuclear NMR spectroscopic studies indicate that $[Fe_4(CO)_{13}(H)]^-$ exists in solution as an equilibrium mixture of two isomers (eq 1).[5] A

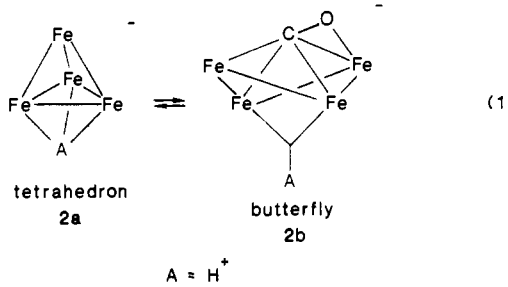

tetrahedron **2a** ⇌ butterfly **2b** (1)

A = H^+

Π-CO such as that in **2b** is postulated to be important in the cleavage of CO on metal surfaces,[6] and it is demonstrated that in acid solution the Π-CO in **2b** is cleaved and converted to CH_4.[7]

In view of the chemically and structurally interesting aspects of **2**, a study was undertaken in this laboratory to determine the factors that lead to the formation of a butterfly structure such as **2b**. In previous research we found that equilibria analogous to eq 1 can be established when a variety of Lewis acids are used in place of the proton. For the Lewis acids employed in that research, A = H^+, $[HgCH_3]^+$, $[AuPR_3]^+$, and $[CuPR_3]^+$, it was concluded that butterfly formation is promoted by electronic factors such that the strongest acid produces the highest concentration of the butterfly isomer.[8] In the present research we have explored the influence of steric factors on equilibrium 1 by increasing the bulk of the Lewis acids, A = $[HgMo(CO)_3Cp]^+$ and $[HgFe(CO)_2Cp]^+$, and have examined the influence of temperature on the equilibrium. The Hg atom in $[HgM(CO)_nCp]^+$ is known to bridge the edge or to cap the face of a transition-metal cluster.[9]

Experimental Section

Materials and Methods. All reactions were performed under an atmosphere of prepurified N_2 by using standard Schlenk techniques.[10] Transfer of solids was carried out in a Vacuum Atmospheres glovebox under N_2, except for the relatively air-stable compounds $(C_5H_5)M(CO)_nHgCl$ (M = Fe, n = 2; M = Mo, n = 3). Solvents were distilled under N_2 from appropriate drying agents: CH_2Cl_2 from P_2O_5, Et_2O from sodium benzophenone, and MeOH and Me_2CHOH from Mg/I_2.

The starting materials $[PPN]_2[Fe_4(CO)_{13}]$ and $(C_5H_5)M(CO)_nHgCl$ (M = Fe, n = 2; M = Mo, n = 3) were prepared by using procedures in the literature.[11,12] The reagents [PPN]Cl (Alfa, $[PPN]^+$ = bis(triphenylphosphine)nitrogen(1+)), $[(C_5H_5)Mo(CO)_3]_2$ (Strem), $[(C_5H_5)Fe(CO)_2]_2$ (Aldrich), $HgCl_2$ (B & A), and $TlPF_6$ (Strem) were used as received. $Fe(CO)_5$ (Alfa) was filtered before use. The ^{13}CO-enriched products were prepared from $[PPN]_2[Fe_4(CO)_{13}]$ that had been enriched to approximately 25% ^{13}CO by exposure to ^{13}CO gas (Mound Labs, 99% ^{13}CO) for a period of 6-7 days. NMR spectra were recorded on a Varian XL400 (^1H, 399.95 MHz) or on a JEOL FX90Q spectrometer (^1H, 89.55 MHz; ^{13}C, 22.49 MHz; ^{199}Hg, 15.97 MHz); the ^{199}Hg spectra were referenced to an external 0.2 M CH_3HgCl solution in $CDCl_3$. Solvents for the NMR measurements were CD_2Cl_2 (Aldrich, 99.5 atom % D) and $(CD_3)_2CO$ (Aldrich, 99.75 atom % D) that had been dried over P_2O_5 and molecular sieves, respectively, and then vacuum-distilled prior to use. In an attempt to retain the configuration of the cluster ion in solution, the crystalline solid was loaded into an NMR tube and cooled to -80 °C in a dry ice-acetone bath and the appropriate solvent, also cooled to -80

(1) (a) Hieber, W.; Sonnekalb, F.; Becker, E. *Chem. Ber.* **1930**, *63*, 973-986. (b) Hieber, W.; Becker, E. *Chem. Ber.* **1930**, *63*, 1405-1417.
(2) Hieber, W.; Werner, R. *Chem. Ber.* **1957**, *90*, 286-296.
(3) (a) Doedens, R. J.; Dahl, L. F. *J. Am. Chem. Soc.* **1966**, *88*, 4847-4855. (b) van Buskirk, G.; Knobler, C. B.; Kaesz, H. D. *Organometallics* **1985**, *4*, 149-153.
(4) Manassero, M.; Sansoni, M.; Longoni, G. J. *J. Chem. Soc., Chem. Commun.* **1976**, 919-920. Manassero, M. private communication.
(5) Horwitz, C. P.; Shriver, D. F. *Organometallics* **1984**, *3*, 756-758.
(6) Muetterties, E. L.; Stein, J. *Chem. Rev.* **1979**, *79*, 479-490.
(7) (a) Whitmire, K. H.; Shriver, D. F. *J. Am. Chem. Soc.* **1980**, *102*, 1456-1457. (b) Whitmore, K. H.; Shriver, D. F. *J. Am Chem. Soc.* **1981**, *103*, 6754-6757. (c) Drezdzon, M. A.; Whitmire, K. H.; Bhattacharyya, A. A.; Hsu, W. L.; Nagel, C. C.; Shore, S. G.; Shriver, D. F. *J. Am. Chem. Soc.* **1982**, *104*, 5630-5633.
(8) (a) Horwitz, C. P.; Holt, E. M.; Brock, C. P.; Shriver, D. F. *J. Am. Chem. Soc.* **1985**, *107*, 8136-8146. (b) Horwitz, C. P.; Shriver, D. F. *J. Am. Chem. Soc.* **1985**, *107*, 8147-8153.
(9) (a) Ermer, S.; King, K.; Hardcastle, K. I.; Rosenberg, E.; Lanfredi, A. M. M.; Tiripicchio, A.; Camellini, M. T. *Inorg. Chem.* **1983**, *22*, 1339-1344. (b) Braunstein, P.; Rosé, J.; Tiripicchio, A.; Camellini, M. T. *J. Chem. Soc., Chem. Commun.* **1984**, 391-392.
(10) Shriver, D. F.; Drezdon, M. A. *The Manipulation of Air-Sensitive Compounds*, 2nd ed.; Wiley: New York, 1986.
(11) Whitmire, K. H.; Ross, J.; Cooper, C. B.; Shriver, D. F. *Inorg. Synth.* **1982**, *21*, 66-69.
(12) (a) King, R. B.; Stone, F. G. A. *Inorg. Synth.* **1963**, *7*, 99-115. (b) Mays, M. J.; Robb, J. D. *J. Chem. Soc. A* **1968**, 329-332 and references cited therein.

0020-1669/88/1327-0552$01.50/0

Table I. Crystal Data for the X-ray Diffraction Measurement of $[PPN][Fe_4(CO)_{13}(HgMo(CO)_3Cp)]$

formula	$C_{57}H_{35}Fe_4HgMoO_{16}NP_2$
fw	1571.77
cryst dimens, mm	0.38 × 0.30 × 0.18
cryst syst	triclinic
space group	$P\bar{1}$
a, Å	16.174 (4)
b, Å	18.457 (4)
c, Å	10.995 (2)
α, deg	100.22 (2)
β, deg	105.57 (2)
γ, deg	64.77 (2)
V, Å^3	2853 (3)
d_{calcd}, g·cm^{-3}	1.83
Z	2
μ(Mo Kα), cm^{-1}	40.88
radiation used	graphite-monochromated Mo Kα (λ = 0.71069 Å)
scan type	$\omega/2\theta$
2θ range, deg	4–50
scan width	0.9 + 0.35 tan θ
temp, °C	−120
total no. of data	10362
no. of unique data, $I > 3\sigma(I)$	8365
no. of params	559
R	0.036
R_w	0.051

°C, was introduced. The sample tube was then quickly transferred to the precooled NMR probe, and the spectrum was obtained on the sample at −80 °C. The NMR spectra confirmed the presence of a single isomer under these conditions. Infrared spectra were recorded on a Perkin-Elmer 283 or 399 spectrophotometer or on a Nicolet 7199 Fourier-transform infrared spectrophotometer, on CH_2Cl_2 solutions or on Fluorolube mulls. Elemental analyses were performed by Analytische Laboratorien Elbach, Engelskirchen, West Germany.

Synthesis of $[PPN][Fe_4(CO)_{13}(HgMo(CO)_3Cp)]$. A sample of 300 mg of $[PPN]_2[Fe_4(CO)_{13}]$ (0.18 mmol), together with 63 mg of $TlPF_6$ (0.18 mmol), was dissolved in 10 mL of CH_2Cl_2, and $(C_5H_5)Mo(CO)_3HgCl$ (89 mg, 0.19 mmol) was then added. After the mixture was stirred for 10 min, the infrared spectrum revealed that the strong absorption for $[Fe_4(CO)_{13}]^{2-}$ at 1948 cm^{-1} had disappeared and a new feature had grown in which consists of several maxima centered at 1998 cm^{-1}, indicating formation of the anion $[Fe_4(CO)_{13}(HgMo(CO)_3Cp)]^-$ (**3**). CH_2Cl_2 was removed under vacuum, 10 mL of Et_2O was added, and TlCl and $[PPN]PF_6$ were removed by filtration. To the filtrate was added 20 mL of isopropyl alcohol. The volume of this solution was reduced to approximately 20 mL by slow evaporation under reduced pressure. When this solution stood at −20 °C for at least 12 h, dark gray crystals with a metallic luster formed. The crystals were collected by filtration, washed with a small amount of isopropyl alcohol, and dried under vacuum. A typical isolated yield was 235 mg (0.15 mmol, 83% based on the starting $[PPN]_2[Fe_4(CO)_{13}]$).

Solution IR (CH_2Cl_2): ν_{CO} 2055 (w), 2020 (s), 1998 (vs), 1980 (sh), 1940 (sh), 1899 (m), 1880 (m) cm^{-1}. The absorption frequencies shift very little upon changing the solvent to MeOH, Et_2O, or THF. Solid-state IR (Fluorolube): ν_{CO} 2055 (w), 2015 (vs), 1998 (vs), 1973 (vs), 1963 (sh), 1945 (m), 1935 (m), 1905 (sh), 1895 (s), 1869 (s), 1418 (m), 1405 (w), 1385 (w) cm^{-1}. ^{1}H NMR (CD_2Cl_2): δ 5.24 (s, 5 H), 7.42 (br m, 30 H). ^{199}Hg NMR (CD_2Cl_2, −80 °C): δ 927.4 (s). ^{13}C NMR (CD_2Cl_2, Fe–carbonyl region only, −80 °C): δ 281.5 (1 C), 220.8 (1 C), 218.7 (2 C), 216.6 (1 C), 215.6 (2 C), 211.2 (2 C), 209.8 (2 C), 207.0 (2 C). Anal. Calcd for $C_{57}H_{35}O_{16}NP_2Fe_4HgMo$: C, 43.56; H, 2.24; N, 0.89; P, 3.94; Fe, 14.21; Hg, 12.76; Mo, 6.10. Found: C, 43.48; H, 2.35; P, 3.70; Fe, 14.25; Hg, 13.00; Mo, 6.11.

Synthesis of $[PPN][Fe_4(CO)_{13}(HgFe(CO)_2Cp)]$. By the procedure described above, $[PPN]_2[Fe_4(CO)_{13}]$ was allowed to react with $CpFe(CO)_2HgCl$. After 10 min of stirring, the IR spectrum of the reaction solution revealed the formation of $[Fe_4(CO)_{13}(HgFe(CO)_2Cp)]^-$ (**4**). Attempts to isolate the product yielded only oil or noncrystalline solid beads. As a result, spectroscopic data are not available on a pure sample of this compound.

X-ray Data Collection and Structure Determination. A summary of crystal and intensity data is presented in Table I. All X-ray measurements were carried out by using Mo Kα radiation on a CAD4 diffractometer with the crystal held at −120 °C. The intensities of three standard reflections were measured every 3 h of X-ray exposure and showed no significant variation. The data were corrected for Lorentz and polarization effects. The absorption correction was based on ψ scans of six Bragg reflections with the transmission factors ranging from 0.67 to 1.00. All calculations were performed on a VAX 11/730 computer using the TEXSAN crystallographic software package.[13] The structure was solved by direct methods (MITHRIL)[14] and refined by full-matrix least-squares procedures. In the final cycles of refinement anisotropic thermal parameters were employed for all non-hydrogen atoms of the complex anion and the P and N atoms of the $[PPN]^+$ cation. The phenyl carbon atoms were refined isotropically. Contributions from the phenyl hydrogen atoms in estimated positions were included in the final cycles of the refinement. The function minimized was $\sum w(|F_o| - |F_c|)^2$ with weights $w = 1/\sigma^2(F)$. No unusual trends were observed in an analysis of the function vs either $(\sin\theta)/\lambda$ or $|F_o|$. The goodness of fit was 2.43. The largest residual peak on the final difference map was 1.6 e/Å^3 high and was located 1.2 Å away from the Fe(4) atom. Atomic scattering factors were those tabulated by Cromer and Waber[15] with anomalous dispersion corrections taken from another table by Cromer.[16] Final coordinates of all the atoms in the anion are reported in Table II.

Table II. Selected Positional Parameters for $[PPN][Fe_4(CO)_{13}(HgMo(CO)_3Cp)]$

atom	x	y	z
Hg	0.36382 (2)	0.30899 (1)	0.06196 (2)
Mo	0.41773 (4)	0.37818 (3)	−0.08930 (5)
Fe(1)	0.34805 (7)	0.10425 (5)	0.14247 (8)
Fe(2)	0.39636 (6)	0.22333 (5)	0.25370 (8)
Fe(3)	0.24066 (6)	0.24640 (5)	0.05861 (8)
Fe(4)	0.22672 (6)	0.32042 (5)	0.18371 (9)
O(11)	0.2592 (5)	0.0028 (4)	−0.0238 (6)
O(12)	0.4631 (4)	0.0878 (3)	−0.0319 (5)
O(13)	0.4851 (4)	−0.0316 (3)	0.2914 (5)
O(21)	0.5850 (4)	0.1553 (3)	0.2029 (6)
O(22)	0.4660 (4)	0.1346 (3)	0.4804 (5)
O(23)	0.4266 (3)	0.3589 (3)	0.4096 (5)
O(31)	0.2702 (5)	0.2097 (3)	−0.2018 (5)
O(32)	0.0916 (4)	0.1876 (4)	−0.0100 (6)
O(33)	0.1084 (3)	0.4116 (3)	0.0025 (5)
O(41)	0.0302 (4)	0.3558 (3)	0.2655 (5)
O(42)	0.2163 (4)	0.4839 (3)	0.2689 (6)
O(43)	0.2706 (4)	0.3091 (4)	0.5569 (5)
O(44)	0.2626 (3)	0.1506 (2)	0.2638 (4)
O(51)	0.4067 (4)	0.4813 (3)	0.1686 (4)
O(52)	0.3453 (4)	0.5523 (3)	−0.1680 (6)
O(53)	0.2075 (4)	0.4112 (3)	−0.2058 (5)
C(11)	0.2903 (6)	0.0446 (4)	0.0406 (7)
C(12)	0.4157 (6)	0.0969 (4)	0.0390 (7)
C(13)	0.4336 (5)	0.0216 (4)	0.2355 (6)
C(21)	0.5091 (5)	0.1822 (4)	0.2159 (7)
C(22)	0.4377 (5)	0.1676 (4)	0.3896 (6)
C(23)	0.4074 (4)	0.3102 (4)	0.3431 (6)
C(31)	0.2633 (5)	0.2219 (4)	−0.0993 (6)
C(32)	0.1508 (5)	0.2095 (4)	0.0188 (7)
C(33)	0.1635 (4)	0.3488 (4)	0.0345 (6)
C(41)	0.1063 (5)	0.3434 (4)	0.2708 (6)
C(42)	0.2202 (5)	0.4208 (4)	0.2725 (7)
C(43)	0.2538 (5)	0.3152 (4)	0.4511 (7)
C(44)	0.2671 (4)	0.2127 (4)	0.2383 (5)
C(51)	0.4101 (5)	0.4406 (4)	0.0763 (6)
C(52)	0.3718 (5)	0.4883 (4)	−0.1394 (7)
C(53)	0.2842 (5)	0.3984 (4)	−0.1578 (6)
C(61)	0.5563 (5)	0.3420 (4)	−0.1570 (8)
C(62)	0.5789 (5)	0.2947 (5)	−0.0341 (7)
C(63)	0.5324 (5)	0.2432 (4)	−0.0921 (8)
C(64)	0.4774 (5)	0.2594 (4)	−0.2179 (8)
C(65)	0.4925 (6)	0.3200 (5)	−0.2587 (7)

Variable-Temperature NMR Measurements. To achieve equilibrium at low temperatures, it was necessary to hold an NMR sample at a desired temperature for time periods that ranged from 5 to 24 h before the spectrum was obtained. At each temperature below room temperature, several spectra were obtained after the equilibration period. The low-temperature slush baths used were[10] chlorobenzene for −45 °C, bromobenzene for −31 °C, tetrachloromethane for −23 °C, diethylene

(13) Swepston, P. N. "TEXSAN; Version 2.0"; Molecular Structure Corp., College Station, TX, 1986.
(14) Gilmore, G. J. "MITHRIL"; University of Glasgow, Glasgow, Scotland, 1983.
(15) *International Tables for X-ray Crystallography*; Kynoch: Birmingham, England, 1974; Vol. 4, pp 99–101.
(16) Reference 15, pp 149–150.

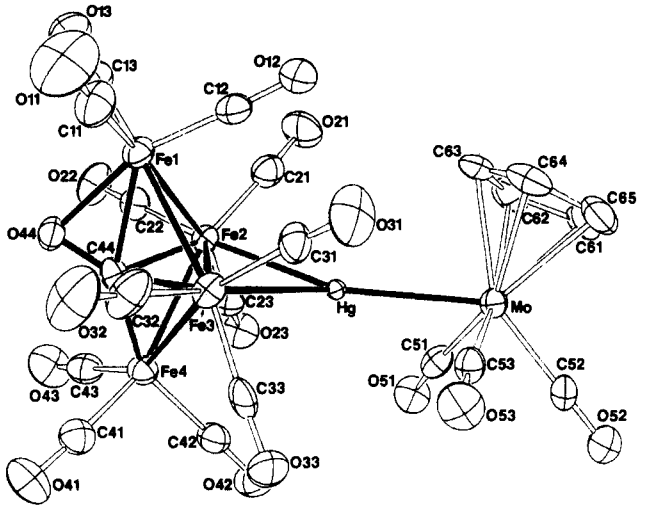

Figure 1. ORTEP diagram of the anion $[Fe_4(CO)_{13}(HgMo(CO)_3Cp)]^-$ (**3b**). Thermal ellipsoids are at the 50% probability level.

glycol for −10 °C, and water for 0 °C. For measurements above room temperature, a freshly dissolved sample was used whenever available and spectra were recorded as soon upon the sample insertion as possible to minimize thermal decomposition.

Results and Discussion

Formation of $[Fe_4(CO)_{13}(HgM(CO)_nCp)]^-$ (3 and 4). The metal cluster anions **3** (M = Mo, n = 3) and **4** (M = Fe, n = 2) were formed under identical conditions, described in the Experimental Section. Although **4** was not isolated as a crystalline solid, both **3** and **4** form readily in solution when $[Fe_4(CO_{13})]^{2-}$ is allowed to react with $CpM(CO)_nHgCl$ (eq 2). The reaction apparently is

$$[Fe_4(CO)_{13}]^{2-} + ClHgM \xrightarrow[CH_2Cl_2]{TlPF_6} [Fe_4(HgM)(CO)_{13}]^- + TlCl + PF_6^- \quad (2)$$

$$M = Mo(CO)_3Cp\ (\mathbf{3}),\ Fe(CO)_2Cp\ (\mathbf{4});\ Cp = C_5H_5$$

driven by the extraction of Cl^- ion by Tl^+ to give insoluble TlCl and, more importantly, the metal basicity[17] of the anionic cluster, $[Fe_4(CO)_{13}]^{2-}$. Formation of the anionic adducts can be monitored by IR spectroscopy, which shows a shift for the strongest CO stretching band of about 55 cm^{-1} toward higher frequency relative to the band for the starting material, $[Fe_4(CO)_{13}]^{2-}$. The $[PPN]^+$ salt of **3** can be isolated by diethyl ether extraction followed by crystallization from isopropyl alcohol. In ether or methanol solution **3** is stable at room temperature for at least 3 h, after which gradual decomposition begins to occur, giving $[Fe_4(CO)_{13}]^{2-}$ and a yellow solid. Infrared spectra indicate that the solid $[PPN]^+$ salt of **3** can be exposed to air for a few days without major decomposition.

Reaction 2 is analogous to those between $[Fe_4(CO)_{13}]^{2-}$ and various Lewis acids such as H^+, $[HgCH_3]^+$, $[AuPR_3]^+$, and $[CuL]^+$.[2,8] Product anions **3** and **4** are the first examples in this series containing bulky Lewis acids.

Single-Crystal Structure of $[PPN][Fe_4(CO)_{13}(HgMo(CO)_3Cp)]$. The structure of this salt was determined by single-crystal X-ray diffraction (see Experimental Section). An ORTEP diagram (Figure 1) is presented for the anion $[Fe_4(CO)_{13}(HgMo(CO)_3Cp)]^-$. Table III summarizes some of the bond distances, bond angles, and dihedral angles.

The Fe_4 moiety has a butterfly framework with Fe(2) and Fe(3) forming the hinge and Fe(1) and Fe(4) the wingtips of the butterfly. We designate the butterfly isomer of $[Fe_4(CO)_{13}(HgMo(CO)_3Cp)]^-$ as **3b**. The dihedral angle between the two wings of the butterfly is 119.75 (5)°, which is greater than that in either the proton adduct $[Fe_4(CO)_{13}(H)]^-$ or the gold adduct $[Fe_4(CO)_{13}(AuPR_3)]^-$ (116.84 and 117.40°, respectively).[4,8] In

Table III. Selected Bond Distances (Å), Angles (deg), and Dihedral Angles (deg) in $[PPN][Fe_4(CO)_{13}(HgMo(CO)_3Cp)]$

(a) Bond Distances

Fe(1)–Fe(2)	2.633 (1)	Hg–Mo	2.7637 (7)
Fe(1)–Fe(3)	2.620 (2)	C(44)–O(44)	1.262 (7)
Fe(2)–Fe(3)	2.763 (1)	Fe(1)–O(44)	1.999 (4)
Fe(2)–Fe(4)	2.633 (2)	Fe(1)–C(44)	2.142 (6)
Fe(3)–Fe(4)	2.623 (1)	Fe(2)–C(44)	2.142 (6)
Hg–Fe(2)	2.664 (1)	Fe(3)–C(44)	2.057 (6)
Hg–Fe(3)	2.686 (1)	Fe(4)–C(44)	1.829 (6)

(b) Bond Angles

Fe(1)–Fe(2)–Fe(3)	58.03 (4)	Fe(1)–C(44)–Fe(4)	153.4 (3)
Fe(1)–Fe(2)–Fe(4)	94.45 (4)	O(44)–C(44)–Fe(1)	66.2 (3)
Fe(1)–Fe(3)–Fe(2)	58.50 (4)	O(44)–C(44)–Fe(4)	140.2 (5)
Fe(1)–Fe(3)–Fe(4)	95.01 (5)	O(44)–Fe(1)–C(44)	35.3 (2)
Fe(2)–Fe(3)–Fe(4)	58.46 (4)	O(44)–Fe(1)–Fe(2)	80.3 (1)
Fe(2)–Fe(4)–Fe(3)	63.43 (4)	O(44)–Fe(1)–Fe(3)	78.6 (1)
Hg–Fe(2)–Fe(1)	103.29 (4)	C(44)–Fe(2)–Fe(1)	52.1 (2)
Hg–Fe(2)–Fe(3)	59.28 (3)	C(44)–Fe(2)–Fe(3)	47.5 (2)
Hg–Fe(2)–Fe(4)	86.71 (4)	C(44)–Fe(2)–Fe(4)	43.5 (2)
Hg–Fe(3)–Fe(1)	103.07 (4)	C(44)–Fe(3)–Fe(1)	52.9 (2)
Hg–Fe(3)–Fe(2)	58.53 (3)	C(44)–Fe(3)–Fe(2)	50.2 (2)
Hg–Fe(3)–Fe(4)	86.48 (4)	C(44)–Fe(3)–Fe(4)	44.0 (2)
Mo–Hg–Fe(2)	153.15 (2)	C(44)–Fe(4)–Fe(2)	53.8 (2)
Mo–Hg–Fe(3)	142.37 (3)	C(44)–Fe(4)–Fe(3)	51.3 (2)

(c) Dihedral Angles

plane 1	plane 2	angle
Fe(1)–Fe(2)–Fe(3)	Fe(4)–Fe(2)–Fe(3)	119.75 (5)
Hg–Fe(2)–Fe(3)	Fe(1)–Fe(2)–Fe(3)	133.32 (4)
Hg–Fe(2)–Fe(3)	C(44)–Fe(2)–Fe(3)	160.9 (2)
Fe(4)–Fe(2)–Fe(3)	C(44)–Fe(2)–Fe(3)	54.0 (2)
Fe(2)–C(44)–Fe(4)	Fe(3)–C(44)–Fe(4)	82.9 (2)
Fe(2)–C(44)–Fe(1)	O(44)–C(44)–Fe(1)	136.9 (4)
Fe(3)–C(44)–Fe(1)	O(44)–C(44)–Fe(1)	137.9 (4)

both the proton and the gold adducts the five Fe–Fe bond distances are nearly equal, but in **3b** the distance between the two hinge Fe atoms is elongated to 2.763 (1) Å, about 0.14 Å longer than the four wingtip-to-hinge Fe–Fe bonds (2.620 (2)–2.633 (2) Å, average 2.627 (6) Å). The II-CO, CO(44), is situated between and above the two wingtip Fe atoms of the butterfly. The C–O bond distance for this II-CO, C(44)–O(44) = 1.262 (7) Å, is equal to the corresponding distances in $[Fe_4(CO)_{13}(H)]^-$ and $[Fe_4(CO)_{13}(AuPR_3)]^-$ (1.26 and 1.254 (9) Å, respectively). C(44) is within bonding distance of all four iron atoms; the closest is a wingtip iron, Fe(4) (1.829 (6) Å). CO(44) is bound to the other wingtip, Fe(1), in an η^2 fashion: C(44)–Fe(1) = 2.142 (6) Å and O(44)–Fe(1) = 1.999 (4) Å. Bonding for all the terminal CO groups, three on each metal, are normal: the C–O bond distances range between 1.130 (8) and 1.178 (9) Å, the Fe–C distances are 1.732 (7)–1.835 (7) Å, and the Mo–C distances are 1.970 (7)–1.978 (7) Å. The M–C–O angles range between 170.3 (6) and 179.7 (7)°. The Mo moiety retains its typical distorted four-legged piano stool configuration with Hg and the three CO's as the legs.[9,18] The Hg atom interacts directly with the Mo atom and the hinge iron atoms, Fe(2) and Fe(3). The $[HgMo(CO)_3Cp]$ group is tilted away from that wingtip which is bound to the oxygen atom of the II-CO ligand (Table III). The Mo–Hg bond is offset from the plane defined by Fe(2), Fe(3), and Hg by about 8° toward the oxo-bound wing:

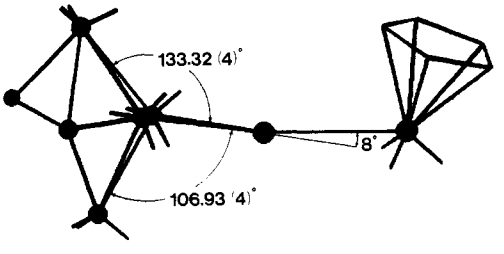

(17) (a) Shriver, D. F. *Acc. Chem. Res.* **1970**, *3*, 231–238 and references cited therein. (b) Werner, H. *Pure Appl. Chem.* **1982**, *54*, 177–188.

(18) Wang, J. M.S. Thesis, California State University, Northridge, CA, Aug 1985, and references cited therein.

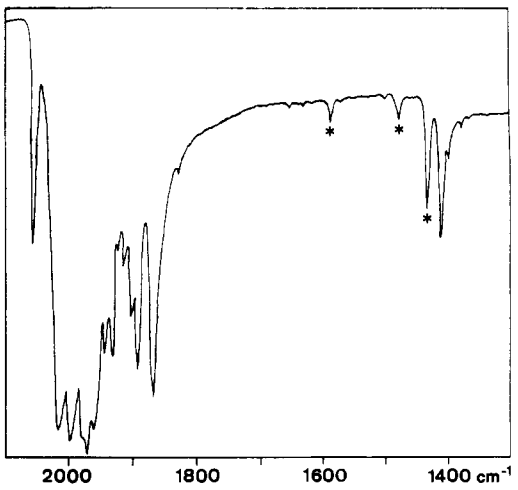

Figure 2. Infrared spectrum of $[PPN][Fe_4(CO)_{13}(HgMo(CO)_3Cp)]$ as a Fluorolube mull between KBr plates. The asterisks denote absorptions by the $[PPN]^+$ cation.

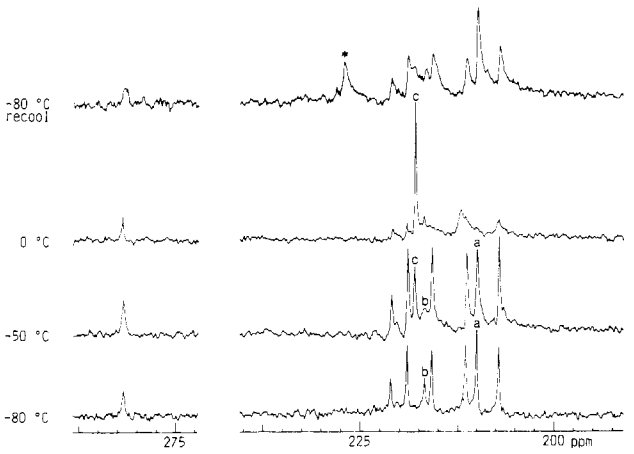

Figure 3. Variable-temperature ^{13}C NMR spectra of ^{13}CO enriched $[PPN][Fe_4(CO)_{13}(HgMo(CO)_3Cp)]$: (bottom) sample dissolved and spectrum recorded at −80 °C; (top) sample cooled *very slowly* to −80 °C after warming to room temperature. The asterisk denotes the resonance due to $[Fe_4(CO)_{13}]^{2-}$ impurity that results from thermal decomposition.

Spectroscopic Characterization of 3. The IR spectrum of solid $[PPN][Fe_4(CO)_{13}(HgMo(CO)_3Cp)]$ (Figure 2) contains absorption maxima at 1417 and 1406 cm^{-1}. One of these is due to the C–C stretching of the cyclopentadienyl group in the Mo moiety.[19] The other is assigned as the stretching frequency of the Π-CO.[5,8] There is no IR band for a conventional C-bridging CO in the 1700–1800-cm^{-1} region. The IR evidence for the presence of a Π-CO and the absence of a μ_2-η-CO in the polycrystalline material is in agreement with the butterfly structure determined by X-ray diffraction on a single crystal.

When crystalline $[PPN][Fe_4(CO)_{13}(HgMo(CO)_3Cp)]$ is dissolved in CD_2Cl_2 at −80 °C and the ^{13}C NMR spectrum run at this temperature, the spectrum (Figure 3) contains a resonance at δ 282.52, which also indicates the presence of a Π-CO.[5,8] Seven other resonances in the region between δ 205 and 225 correspond to twelve terminal carbonyls, consistent with a butterfly cluster of C_s symmetry, **3b**, in which each of the five nonequivalent pairs of CO's are interrelated by the mirror plane, with two terminal CO's and the one Π-CO in the mirror plane. These NMR assignments are consistent with the butterfly structure determined by single-crystal X-ray diffraction.

At −50 °C, two of the terminal ^{13}CO resonances, designated as a and b in Figure 3, start to collapse. In addition, a new resonance, c, appears at δ 217.9, which is not the position for the weighted average of a and b. As the temperature is raised further, a and b coalesce and the other five terminal CO peaks collapse and eventually coalesce also. But resonance c increases in intensity. The a–b exchange pattern indicates a low-energy local rotational process involving three CO's on one of the two wingtip iron atoms, which may be the iron that is not bonded to the oxygen of the Π-CO.[8] The resonance c at δ 217.9 is assigned to the tetrahedral isomer, **3a**, in which all CO ligands are fluxional.[5,8] Above room temperature, another resonance at δ 227.8 is observed, which represents $[Fe_4(CO)_{13}]^{2-}$ from thermal decomposition. When the sample is recooled *very slowly* to −80 °C, the spectrum corresponds to that for a mixture of the butterfly isomer, a small amount of $[Fe_4(CO)_{13}]^{2-}$, and virtually none of the tetrahedral isomer.

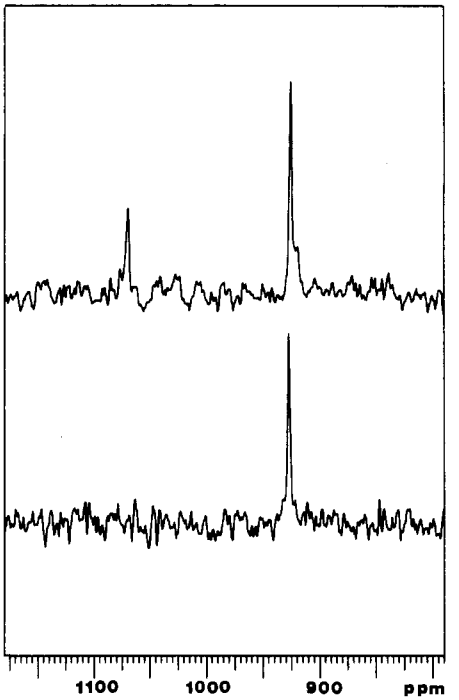

Figure 4. ^{199}Hg NMR spectra of $[PPN][Fe_4(CO)_{13}(HgMo(CO)_3Cp)]$: (bottom) sample dissolved and spectrum recorded at −80 °C; (top) sample warmed to room temperature and then quickly recooled to −80 °C.

The ^{199}Hg NMR spectrum taken on a solution at −80 °C consists of only one singlet at δ 927.4. After the solution is warmed to room temperature and then *quickly* recooled to −80 °C, two singlets are observed at δ 927.4 and 1054.5, with relative intensity 2.3:1, respectively (Figure 4). The δ 1054.5 resonance is assigned to the tetrahedral isomer, **3a**, and the δ 927.4 band to the butterfly, **3b**.[8] Therefore, the isomer ratio is 2.3:1 at some temperature intermediate between 20 and −80 °C. The ^1H NMR spectra also confirm the presence of the butterfly and tetrahedral isomers. The initial spectrum at −80 °C shows one proton resonance for the Cp group at δ 5.59 for **3b** (Figure 5). At 24 °C, two Cp resonances are present at δ 5.59 and 5.54; the relative intensity is approximately 1.6:1, indicating a 1.6:1 ratio of butterfly to tetrahedral isomers at room temperature.

Butterfly to Tetrahedron Ratio for 3. Previous research indicated that the ratio of butterfly to tetrahedron increases in the order $[Fe_4(CO)_{13}]^{2-} < [Fe_4(CO)_{13}(AuPR_3)]^- < [Fe_4(CO)_{13}(HgCH_3)]^- < [Fe_4(CO)_{13}(H)]^-$, which also is the order of increasing CO frequency for the strongest band in the IR spectrum.[8] This monotonic relation between CO stretching frequency and isomer ratio, points a, b, c, and d in Figure 6, was taken as evidence for a predominant role of electronic factors in determining the stability and thus the proportion of the butterfly isomer.[20] In other words, attack on $[Fe_4(CO)_{13}]^{2-}$ by the stronger Lewis acid yields a higher proportion of the butterfly isomer. Furthermore,

(19) Nakamoto, K. *Infrared and Raman Spectra of Inorganic and Coordination Compounds*, 4th ed.; Wiley: New York, 1986.

(20) The value of ν_{CO} is shown by many different studies to be an indicator of the electron density on a metal carbonyl cluster: (a) Shriver, D. F.; Cooper, C. B. III. *Adv. Infrared Raman Spectrosc.*, **1980**, *6*, 127–157. (b) Chini, P. *Inorg. Chim. Acta, Rev.* **1968**, *2*, 31–51.

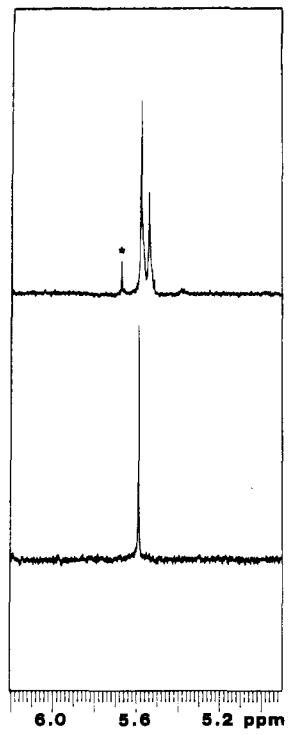

Figure 5. ^1H NMR spectra of $[PPN][Fe_4(CO)_{13}(HgMo(CO)_3Cp)]$: (bottom) sample dissolved and run at −80 °C; (top) sample run at room temperature. The asterisk denotes the signal of a thermal decomposition product.

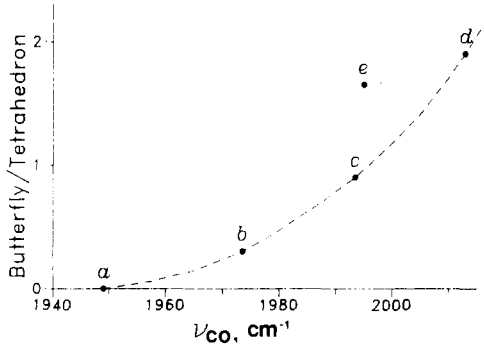

Figure 6. Plot of the butterfly to tetrahedral isomer ratios, determined by NMR spectroscopy, vs the major ν_{CO} frequencies in solutions of (a) $[Fe_4(CO)_{13}]^{2-}$, (b) $[Fe_4(CO)_{13}(AuPR_3)]^-$, (c) $[Fe_4(CO)_{13}(HgCH_3)]^-$, (d) $[Fe_4(CO)_{13}(H)]^-$, and (e) $[Fe_4(CO)_{13}(HgMo(CO_3)Cp)]^-$.

the lack of correlation of isomer ratios with the bulk of acids indicated that steric effects had little, if any, influence on the preference of product isomers in this series.

In the present work, the strongest CO stretching frequency is approximately the same in the three mercury adducts $[Fe_4(CO)_{13}(HgCH_3)]^-$ (1993 cm^{-1}) $[Fe_4(CO)_{13}(HgMo(CO)_3Cp)]^-$ (1995 cm^{-1}) and $[Fe_4(CO)_{13}(HgFe(CO)_2Cp)]^-$ (1997 cm^{-1}). This suggests that the electron density on the cluster is not significantly altered by substituting $[HgM(CO)_nCp]^+$ for $[HgCH_3]^+$, and similar butterfly to tetrahedron ratios would be expected for $[Fe_4(CO)_{13}(HgMo(CO)_3Cp)]^-$ (**3**) and for $[Fe_4(CO)_{13}(HgCH_3)]^-$ (**5**). The actual butterfly to tetrahedral isomer ratio for **3** is 1.6:1, substantially greater than the 0.95:1 ratio for **5** (compare points e and c in Figure 6). Because IR spectra show that $[HgCH_3]^+$ and $[HgMo(CO)_3Cp]^+$ have similar acidity, steric effects are the likely origin for the higher butterfly concentration in **3**. It is conceivable that the bulky $[HgMo(CO)_3Cp]^+$ is better accommodated by the butterfly isomer, since the edge-bridging Hg in the butterfly should be more distant from the Fe_4 moiety than the face-bridging Hg in the tetrahedron. This constitutes a steric contribution that is additional to the electronic factors for promoting butterfly formation.

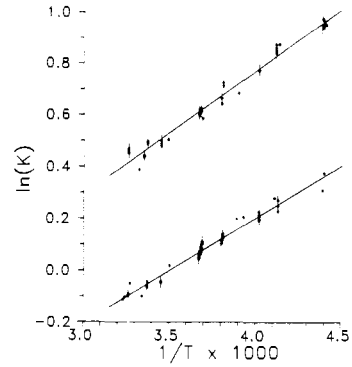

Figure 7. Plot of logarithms of the butterfly to tetrahedral isomer ratios, measured by ^1H NMR spectroscopy, vs reciprocals of the temperatures of measurement: (lower line) $[Fe_4(CO)_{13}(HgCH_3)]^-$ (**5**); (upper line) $[Fe_4(CO)_{13}(HgMo(CO)_3Cp)]^-$ (**3**). Error bars represent sample standard deviations.

Thermodynamics of Isomerization. The integrated intensities were determined for each of the two cyclopentadienyl and the two methyl resonances in the ^1H NMR spectra for **3** and **5**, respectively. In Figure 7, , the logarithm of the intensity ratios is plotted against the reciprocal of the temperatures. Values of $\Delta H°$ and $\Delta S°$ for the tetrahedron to butterfly isomerization of **3** and of **5** were calculated from the slope and intercept of the least-squares line fit to the more than 65 data points for each compound. The $\Delta H°$ value for the conversion of the butterfly to the tetrahedral isomer of **3** is −4.0 ± 0.1 kJ·mol^{-1}. This value is more negative than the $\Delta H°$ value for the corresponding isomerization of **5**, −3.4 ± 0.1 kJ·mol^{-1}. The $\Delta S°$ value for **3**, −9.6 ± 0.2 J·K^{-1}·mol^{-1}, on the other hand, is less negative or more positive than the $\Delta S°$ for **5**, −11.8 ± 0.3 J·K^{-1}·mol^{-1}. The $\Delta H°$ and $\Delta S°$ values for the two different compounds differ by substantially more than 3σ. Both $\Delta H°$ and $\Delta S°$ vary in the direction that favors a higher proportion of the butterfly isomer for **3** over that for **5**.

Molecular Mechanics. Rigorous application of molecular mechanics to the present cluster systems is limited by the lack of empirical potential energy functions for all of the bond stretchings, bond deformations, and nonbonding interactions. The problem is complicated further by the lack of structural parameters for some of the isomers. Nonetheless, molecular mechanical treatment in which calculations are based on ligand–ligand repulsions for model structures may provide some insight into the isomerization process. Such approaches have been used previously to rationalize the tetrahedral metal skeleton of $[M_4(CO)_{13}]^{2-}$ clusters,[21] to infer the reactivity of $[Fe_4(CO)_{13}(H)]^-$ toward the methyl carbocation,[22] and to describe the disposition of carbonyl ligands in metal clusters.[23]

Because of the lack of single crystals for some of the isomers, X-ray structures are known only for the tetrahedral $[Fe_4(CO)_{13}(HgCH_3)]^-$ (**5a**)[8] and the butterfly $[Fe_4(CO)_{13}(HgMo(CO)_3Cp)]^-$ (**3b**) but not for the butterfly $[Fe_4(CO)_{13}(HgCH_3)]^-$ (**5b**) or the tetrahedral $[Fe_4(CO)_{13}(HgMo(CO)_3Cp)]^-$ (**3a**). We constructed models for **3a** and **5b** from the fragments of the known structures of **3b** and **5a**, as illustrated in Figure 8. The model of **3a** contains the tetrahedral $[Fe_4(CO)_{13}Hg]$ from **5a** and the $[Mo(CO)_3Cp]$ fragment from **3b**. The configuration of all the ligands in each fragment was preserved. In connecting the two portions, the Hg–Mo bond retained the orientation of the Hg–C bond relative to the Fe_4 framework in **5a** and the orientation of the Hg–Mo bond relative to the Mo moiety in **3b**; the Hg–Mo bond distance remained identical with that in **3b**, 2.7637 Å. The other model molecule, **5b**, was generated by replacing the $[Mo(CO)_3Cp]$ moiety of **3b** with a methyl group from the standard

(21) Horwitz, C. P.; Holt, E. M.; Shriver, D. F. *Inorg. Chem.* **1984**, *23*, 2491–2499.
(22) Bogdan, P. L.; Horwitz, C. P.; Shriver, D. F. *J. Chem. Soc., Chem. Commun.* **1986**, 553–555.
(23) (a) Benfield, R. E.; Johnson, B. F. G. *J. Chem. Soc., Dalton Trans.* **1980**, 1743–1767. (b) Lauher, J. W. *J. Am. Chem. Soc.* **1986**, *108*, 1521–1531 and references cited therein.

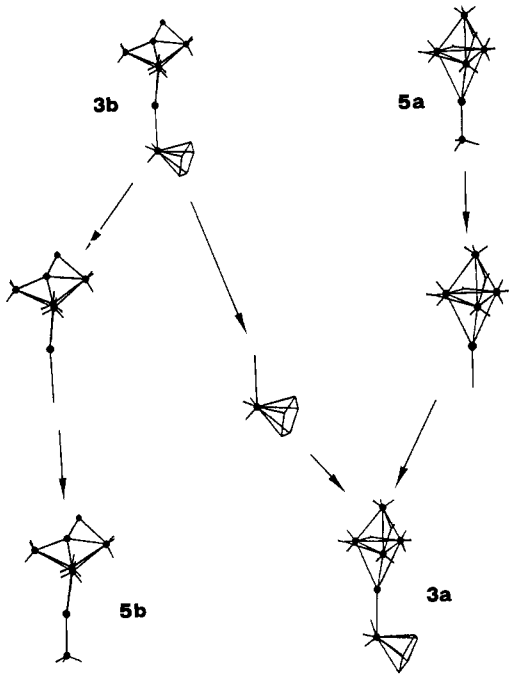

Figure 8. Scheme of construction of models **3a** and **5b** from the known crystal structures of **3b** and **5a**. Terminal CO ligands are reduced to short sticks for clarity.

structural fragment library of the CHEMGRAF program.[24] The Hg–C vector was constrained to coincide with the Hg–Mo vector in **3b**, and the length of the Hg–C bond, 2.134 Å, was taken from **5a**. By use of CHEMGRAF, partial minimization of ligand repulsion was performed with respect to rotation around each of the newly formed bonds.

Inspection of the nonbonded distances in the crystal structure of **3b** reveals close contacts between the hydrogen atoms on the Cp ring and the CO groups on the Fe_4 cluster and between the Mo–CO groups and the Fe–CO groups. Some of the short nonbonding distances are as follows (Å): H(63)–O(12) = 2.744, H(63)–O(21) = 2.728, H(64)–O(31) = 3.062, O(53)–O(33) = 3.098. The corresponding distances in the simulated tetrahedron, **3a**, are relatively longer (Å): H(63)–O(22) = 3.665, H(63)–O(31) = 3.698, H(62)–O(31) = 3.292, O(51)–O(41) = 3.280, O(53)–O(41) = 3.313. See structure **3a** for atom positions. From

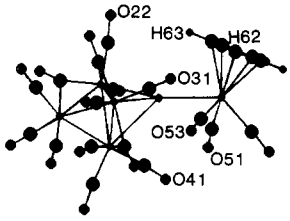

3a

this comparison, it appears that the tetrahedral form of $[Fe_4(CO)_{13}(HgMo(CO)_3Cp)]^-$, **3a**, should be more stable than the butterfly isomer, **3b**. This is contrary both to the experimental observations and to intuition.

A qualitative assessment of the ligand–ligand repulsion in **3a** vs **3b** and **5a** vs **5b** was performed by using the CHEMGRAF program. The structures known from crystallography, **3b** and **5a**, and the model structures **3a** and **5b**, were employed for the calculations. The van der Waals repulsion energy between nonbonded CO and Cp ligands in **3a** is 64.8 kJ·mol^{-1} greater than in **3b**. The corresponding energy difference between **5a** and **5b** is 65.4 kJ·mol^{-1}. This implies that the butterfly form is favored in $[Fe_4(CO)_{13}(HgCH_3)]^-$ (**5**) by 0.6 kJ·mol^{-1} over that in the cluster with the bulky Lewis acid ligand $[Fe_4(CO)_{13}(HgMo(CO)_3Cp)]^-$ (**3**). Again this result is contrary to both intuition and experiment; presumably the model structures are inappropriate. It is impractical to perform a total energy minimization for both the butterfly and tetrahedral structures, because we lack necessary data on potential functions for metal–metal and metal–ligand stretch and bond angle deformation.

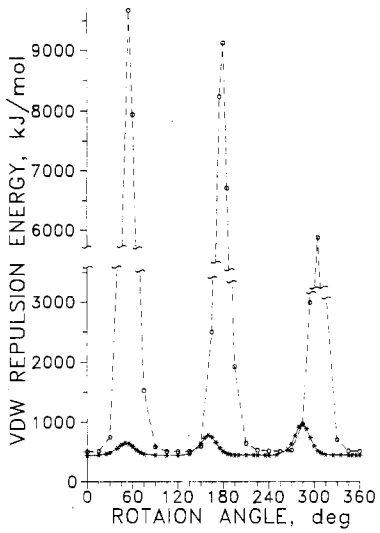

Figure 9. Plot of the ligand repulsion energy values, calculated by CHEMGRAF, vs the angles of rotation of the Mo moiety relative to the Fe_4 moiety in (asterisks, solid line) **3b** and (open circles, dashed line) **3a**.

In order to interpret the greater entropic term for the equilibrium between the tetrahedral **3a** and butterfly **3b**, we examined the barriers to rotation of the $[Mo(CO)_3Cp]$ moiety around the Hg–Mo bond while holding the Fe_4 moiety fixed. As illustrated in Figure 9, the differences between potential energy profiles, as given by CHEMGRAF, for **3a** and for **3b** are large, with the tetrahedral form **3a** having much more hindered rotation. Although the energy barriers in this figure are unrealistically high due to the absence of ligand flexibility in our model, the two energy profiles qualitatively indicate that **3b** has a greater internal rotational freedom and thus a higher entropy than does **3a**. The rotation of the methyl group about the Hg–C bond in both **5a** and **5b**, on the other hand, is almost completely free. This result is qualitatively sensible, and it is in agreement with the favorable $\Delta S°$ for the conversion of tetrahedron to butterfly, **3a** to **3b**, from the experiments.

Conclusion. Comparisons of the butterfly to tetrahedral isomer ratios with CO stretching frequencies for a series of $[Fe_4(CO)_{13}(A)]^-$ clusters indicate that with relatively compact Lewis acids, H^+, $[CuPPh_3]^+$, $[AuPPh_3]^+$, and $[HgCH_3]^+$, electronic factors control the ratios of butterfly to tetrahedral isomers in solution. When the bulky acid $[HgMo(CO)_3Cp]^+$ is coordinated to $[Fe_4(CO)_{13}]^{2-}$, steric factors appear to favor the more open butterfly adduct. The change of the isomer ratio as a function of temperature shows that this steric phenomenon consists of contributions from enthalpy as well as entropy terms, both favoring more butterfly in **3** and less in **5**. Molecular mechanics calculations indicate that the entropy contribution may originate from the rotation of the Lewis acid ligand. However, the repulsion energies calculated for the butterfly and tetrahedral isomers are not in agreement with the sign of the experimental enthalpy of isomerization.

Acknowledgment. J.W. thanks Cynthia K. Schauer, Paula Bogdan, and Ralph Spindler for helpful suggestions. This research was supported by the NSF Synthetic Inorganic and Organometallic Chemistry Program.

Supplementary Material Available: For $[PPN][Fe_4(CO)_{13}(HgMo(CO)_3Cp)]$, listings of thermal parameters, additional positional parameters for the $[PPN]^+$ cation, and additional bond distances, bond angles, and torsion angles (23 pages); complete listings of observed and calculated structure factors (57 pages). Ordering information is given on any current masthead page.

(24) Davies, E. K. "CHEMGRAF Program Suite"; Chemical Crystallography Laboratory, University of Oxford, Oxford, England, 1984.